Adsorption of REE(III)-humate complexes onto MnO2: Experimental evidence for cerium anomaly and lanthanide tetrad effect inhibition

Mélanie Davranche, Olivier Pourret, Gérard Gruau, Aline N. Dia, Martine Bouhnik-Le Coz

Adsorption of REE(III)-humate complexes onto MnO_2: Experimental evidence for cerium anomaly and lanthanide tetrad effect inhibition

Mélanie Davranche*, Olivier Pourret, Gérard Gruau, Aline Dia, Martine Le Coz-Bouhnik

CAREN, Géosciences Rennes, UMR CNRS 6118, Campus de Beaulieu

35042 RENNES Cedex, France

Abstract- Adsorption experiments of rare-earths elements (REE) onto MnO_2 have been conducted to evaluate the effects of REE organic complexation on both REE(III) adsorption kinetics and Ce(III) oxidation rates. Two types of aqueous solutions - NaCl and $NaNO_3$ - were tested at pH 5 and 7.5. REE(III) adsorption kinetics and Ce(III) oxidation rates is evidenced to depend strongly on REE speciation. Time-series experiments indicate that a stationary exchange equilibrium is reached within less than 10 h when dissolved REE(III) occurs as free species whereas steady state is not reached before 10 d when REE occur as REE-humate complexes. Humate complexation also results in an inhibition of positive Ce anomalies and M-type lanthanide tetrad effect development in REE patterns. Monitoring of dissolved organic carbon (DOC) concentrations showed that ratios of $\log K_d^{REE_{organic}} / \log K_d^{DOC}$ ratios were close to 1.0, implying that the REE(III) and humate remained bound to each other.

The lack of Ce anomaly development when REE occurred as REE-humate complexes seems to arise from the humate shielding of the MnO_2 surface and Ce(IV) preferential adsorption inhibition. The suppression of the lanthanide tetrad effect suggests that REE(III)-humate complexes is bound to MnO_2 by the humate side (anionic adsorption). Thus, Ce cannot be used as a reliable proxy of redox conditions, in either organic-rich waters, or precipitates formed at equilibrium with organic-rich waters. Furthermore, they explain why despite the

Author to whom correspondence should be addressed
(melanie.davranche@univ-rennes1.fr)

development of strongly oxidizing conditions and the presence of MnO_2 in the aquifer, no (or insignificant) negative Ce anomalies are observed in organic-rich waters.

Key-words-Ce anomaly, REE, humic acid, Mn oxide, scavenging-oxidation, ternary surface complex.

1. INTRODUCTION

Studies of the behaviour of the rare earth elements (REE) have recently become an essential part of aqueous trace element chemistry. The reason for this is that REE represent a very coherent group of elements whose chemical properties vary gradually along the group. They exhibit similar chemical properties, which vary gradually along the group and are a highly sensitive to pH, sorption processes changes and strongly influenced by redox chemistry of Fe and Mn. Thus, they have been used as tracers in studies dedicated to the geochemistry of rivers, lakes, seawater, groundwater and geothermal fluids (Elderfield and Greaves, 1982; De Baar et al., 1983, 1985, 1988; Elderfield, 1988; Elderfield et al., 1990; Smedley et al. 1991; Gosselin et al., 1992; Johannesson and Lyons, 1994, 1995; Johannesson et al., 1995; Braun et al. 1998; Van Middlesworth and Wood, 1998; Elbaz-Poulichet and Dupuy, 1999; Dia et al., 2000; Leybourne et al., 2000; Yan et al., 2001; Aubert et al., 2002; Biddau et al., 2002; Möller et al., 2002). One of the major conclusions of these studies is that Ce can be fractionated from the remaining dissolved REE as revealed by the widespread occurrence of negative Ce anomalies in both oceanic and fresh waters. Seawater, for example, show a strong negative Ce anomaly which is mirrored by a positive anomaly in hydrogenic ferromanganese nodules (Piper 1974; Elderfield et al., 1981; De Carlo and McMurthy 1992). Groundwaters also show frequently negative Ce anomalies (Smedley et al. 1991; Braun et al.

1998; Dia et al., 2000; Leybourne et al., 2000). These studies evidence also that REE in solution (river, ground and soil waters) are generally not truly dissolved REE but correspond to colloidal-borne REE (Sholkovitz, 1995; Viers et al., 1997).

REE exhibit a (+III) oxidation state in natural environments. However, among REE, Ce can occur in oxidizing conditions as Ce(IV). Ce oxidation can occur abiotically through oxidation/scavenging of dissolved Ce(III) by Mn and Fe oxyhydroxides (De Carlo et al., 1998; Bau, 1999; Ohta and Kawabe, 2001), or biotically by microbially-mediated redox reactions (i) bacteria oxidize directly Ce(III) into Ce (IV), or (ii) bacteria oxidize Mn(II) into Mn(IV), the Mn oxyhydroxide formed using as an oxidation surface for Ce(III) (Moffet, 1990). Because Ce(IV) is adsorbed more strongly than the other trivalent REE, the Ce(III) oxidation/scavenging reaction may result in solutions displaying a negative Ce anomaly,whereas the solids exhibit positive Ce anomalies. This feature has been largely used for geochemical fingerprinting of redox conditions and notably in the study of marine environments (De Baar et al., 1983, 1985, 1988; Elderfield, 1988; Smedley et al. 1991; Johannesson and Lyons, 1994, 1995; Braun et al. 1998; Leybourne et al., 2000; Kuss et al., 2001) or paleo-environments (Wright et al., 1987; Macleod and Irving, 1996; Holser, 1997; Morad and Felitsyn, 2001).

Much attention has also been paid in recent years to the potential application of Ce anomaly as either, a paleo-oceanographic indicator of widespread marine anoxia, or as a redox proxy in paleosols (Wright et al., 1987; Macleod and Irving, 1996; Gallet et al., 1996; Holser, 1997; Morad and Felitsyn, 2001; Picard et al., 2002).

However, many oxidizing waters do not exhibit negative Ce anomalies. In fact, evidence exists that the occurrence of organic ligands in the solutions may prevent Ce(III) oxidation. Such evidence was provided by Dia et al. (2000) who reported time-series data for REE, dissolved organic carbon (DOC) (DOC content ranging from 7 to 32 $mg.L^{-1}$), Fe, and

Mn concentrations for organic-rich, shallow groundwater from a small catchments in western France. Despite the development of temporary oxidizing conditions and neoformation of Mn oxides, no (or insignificant) negative Ce anomalies were observed ($\Omega(Ce)>0$). Similar results were reported by Viers et al. (1997) who investigated the major, trace element and REE chemistry of organic-rich shallow groundwaters from a small tropical catchments in western Africa. In such organic-rich, shallow groundwaters, the so-called "dissolved" REE pool generally occurs as REE(III)-humate complexes (Viers et al., 1997). This observation is consistent with the high conditional stability constants of these complexes (Byrne and Li, 1995; Takahashi et al., 1997, 1999). These studies strongly suggest that complexation of REE by humic substances might be the key factor that prevents oxidative scavenging of Ce(III) in these waters.

Understanding the sensitivity of REE(III) sorption properties and Ce(III) oxidation rates to REE(III) speciation is especially important since Ce anomaly has often been proposed as paleoredox proxy, both in the ocean and in soils. This application certainly has potential, but requires a more thorough understanding of the processes that control the oxidation and reduction of Ce in both the marine and continental environments. The aim of this study is to compare apparent REE distribution coefficients and apparent Ce(III) oxidation rates from MnO_2 suspensions in which the REE(III) occurred alternatively as REE(III)-humate complex and free REE(III) inorganic species.

2. EXPERIMENTAL SET UP

All chemicals used in this study were of analytical grade. All solutions were prepared with doubly de-ionized water (Milli-Q system, Millipore). The polyethylene containers used in the adsorption experiments were soaked in 10% Ultrapure HNO_3 for 48 h at 60°C, then

rinsed with Milli-Q water for 24 h at 60°C, to remove all possible REE contamination sources. Synthetic REE solutions were prepared from nitrate REE standards (10 ppm; Accu Trace^{TM} Reference Standard). REE concentrations were determined by ICP-MS – HP 4500, Agilent Technologies – at Rennes University (Appendix 1).

2.1. Manganese oxide

Synthetic MnO_2 (Aldrich) was used in the adsorption-oxidation experiments. The solid structure was analyzed by X-Ray diffraction (XRD) on a Siemens D5000 diffractometer. The principle *d* spacing indicated a pyrolusite (MnO_2) structure. The total surface site number of MnO_2 was estimated using the solid CEC (Cation Exchange Capacity) and determined following the cobalthexammine method, ISO 11260 (AFNOR, 1994). Ions bound with the solid surface are exchanged with cobalthexammine ions, and the CEC is the concentration of cobalthexammine ions eliminated from the solution. Five g of solid MnO_2 were mixed with 10 mL of 0.017 M cobalthexammine solution for 3 h. The suspension was then centrifuged and the concentration of cobalthexammine ion remaining in the solution was measured at 470 nm with a Shimadzu-160 A U.V.-spectrophotometer. These analyses indicate that this MnO_2 has a CEC of 70 meq/100g.

Surface acidity constants were determined from potentiometric titrations of 5 $g.L^{-1}$ of solid with NaOH (0.1 M) and HNO_3 (0.1 M) in 0.1 M NaCl solution as the supporting electrolyte (Davranche et al., 2002). Titrations were carried out with a Metrohm 794 DMS Titrino apparatus equipped with a Metrohm combined (3 M KCl) glass electrode. Acidity constants obtained are pK_{a1} 7.89 and pK_{a2} 3.65 and pHzpc is equal to 5.8, a value that falls within the reported pH_{zpc} range of MnO_2 (ie. 4.5 to 7.8; Langmuir, 1997).

2.2. REE(III)-humate complexes

Humate, referred to below as humate (purified humic acid), was obtained from the synthetic Aldrich humic acid (Aldrich, H1,675-2) according to the process described by Vermeer et al. (1998). The humate obtained in this way is ash free and in its protonated form, with the following elemental composition (in weight percent): C = 55.8%, O = 38.9%, H = 4.6%, N = 0.6%. Purified humic acid has a mean molecular weight of 23 000 Daltons (Vermeer et al., 1998). Prior to use, the freeze-dried humate was resuspended overnight in a NaOH solution (pH 10) to ensure complete dissolution of the sample.

Rare-earth element-humate complexes were prepared as follows. Twenty mg of dissolved humate were enclosed in a 250-mL sodium-acetate dialysis bag with a pore size of 12 000-14 000 Daltons. The bag was introduced into 1000 mL of a 5 ppb REE solution, the ionic strength being fixed at 10^{-3} M with NaCl or $NaNO_3$ and the pH adjusted to 7 with HNO_3. Both NaCl and $NaNO_3$ were used as neutral electrolytes. The suspension was stirred for 48 h (equilibrium time determined from preliminary kinetic experiments), to allow equilibration and partitioning of the REE between the aqueous solution and the humate suspension. The dialysis bag was then removed and the REE- humate complexes recovered. The concentrations of REE in solution both inside and outside the dialysis bag were monitored vs. time in order to quantify the amount of REE complexed to humate. Possible REE adsorption onto the dialysis bag was checked by analysing REE content of the membrane (dissolved by acidic digestion with HNO_3 14 N). The results show that complexation rates increase regularly from the heavy to the light REE, which is consistent with the stability constant order determined by Takahashi et al. (1997) and Tang and Johannesson (2003) for REE(III)-humate complexes. Around 75 to 52 % with NaCl and 95 to 87% with $NaNO_3$ of the REE initially

present in the solution were complexed to the humate. The remaining 25-48 or 5-13 % were left in solution outside the membrane or adsorbed onto the dialysis bag.

2.3. Adsorption procedure

Five time-series experiments (in duplicate or triplicate) were conducted to assess the effects of organic complexation on REE(III) adsorption by MnO_2. All suspension were performed with a 100 $mg.L^{-1}$ MnO_2 and allowed to equilibrate with a 10^{-3} M NaCl or $NaNO_3$ aqueous solution at pH 5 (both inorganic and organic speciation) and 7.5 (organic speciation only). Experiments were carried out at room temperature, i.e. 20°C±2. The pH was monitored periodically with a pH-meter and adjusted to 5 and 7.5 by addition of HNO_3 (4.6 N) or NaOH (4 N). The 5-pH condition was chosen to promote REE adsorption (but to avoid total REE sorption that might mask an eventual Ce anomaly development) and 7.5-pH condition to promote cationic adsorption. The choice of $NaNO_3$ as one of the two tested neutral electrolytes was imposed by the occurrence of high NO_3^- concentrations (up to 5.10^{-3} M) in the organic-rich, shallow groundwaters studied by Dia et al. (2000). In inorganic experiments, solutions were made up from 5 ppb REE and in organic experiments, concentrations were 20 $mg.L^{-1}$ for humate, ≈ 3.8-2.6 ppb with NaCl and ≈ 4.8-4.3 ppb with $NaNO_3$ for REE, respectively (concentration obtained after REE/humate complexation).

The first set of experiments carried out with free REE(III) (5 ppb, corresponding to the molar concentration range of 36 to 29 nM) were conducted to validate the experimental and analytical set-up used in this study. Data concerning inorganic REE(III) scavenging onto MnO_2 already exists in the literature and could be used for comparison (Koeppenkastrop and De Carlo, 1992, 1993; Ohta and Kawabe, 2001). In the other time-series experiments, equilibrations were conducted using the above described REE(III)-humate complexes.

Here, we quantify the adsorption behaviour of the REE by using the apparent partition coefficient K_d, expressed as:

$$K_d = \frac{\mu g\ REE\ adsorbed / g\ Mn\ oxide}{\mu g.L^{-1}\ REE\ in\ solution} \quad (1)$$

Ce anomalies are quantified using the Ω(Ce) notation (Grandjean et al, 1987) where:

$$\Omega(Ce) = \left(\log K_d^{Ce} / \sqrt{\log K_d^{La}} / \sqrt{\log K_d^{Pr}} \right) - 1) \quad (2)$$

Suspension aliquots of about 10 mL were regularly sampled and filtrated through 0.2 μm cellulose acetate filters (Sartorius) and the REE concentrations analysed to determined K_d variations through time. Sample aliquots used for REE determination were all immediately digested with suboiled nitric acid (HNO_3 14 N) at 100°C, then resolubilized in HNO_3 0.4 N after complete evaporation, in order to avoid interferences with organic matter during mass analysis for the organic experiments. Precisions on REE concentrations and $\log K_d^{REE}$ values of individual experiments are estimated at ±2% (Appendix 1). Duplicate and triplicate experiments show that the overall reproducibility of the $\log K_d^{REE}$ values is better than ±10% (Appendix 2).

The adsorption behaviour of the REE(III)-humate complexes was also monitored by measuring the dissolved organic carbon (DOC) content of the experimental solutions. DOC measurements can be converted into apparent partition coefficients using Eqn. (3):

$$K_d = \frac{\mu g\ DOC\ adsorbed / g\ Mn\ oxide}{\mu g.mL^{-1}\ DOC\ in\ solution} \quad (3)$$

Dissolved organic carbon concentrations were determined at Rennes University using a Shimadzu 5000 TOC analyzer. Precision and reproducibility are estimated at ±1.5% and ±10%, respectively (Appendix 2).

3. RESULTS

3.1. Adsorption of inorganic REE(III)$_{(aq)}$

The experimental results of Log K_d for La, Ce, Pr and Sm are plotted vs. time in Fig. 2. The values were almost constant over 10 h to 12 d, NaCl run exhibiting a faster adsorption as compared with those conducted with $NaNO_3$. The data point to the same conclusion to that reached by Ohta and Kawabe (2001), namely, that steady state is attained within less than one d (<10 h, here) when REE occur in the solution as free inorganic species, a result which was already apparent in the works of Koeppenkastrop and De Carlo (1992, 1993). The discrepancy between the equilibrium K_d values obtained here and those reported by Ohta and Kawabe (2001) appears to be a direct consequence of the lower MnO_2 concentration used in our experiment: ~100 mg.L^{-1} against 3.2 mg.L^{-1} in Ohta and Kawabe (2001).

All patterns exhibit large positive Ce anomalies (Figs. 3 and 6) as well as convex tetrad curves or "M" shape, two features already evidenced by Ohta and Kawabe (2001). The tetrad effect corresponds to small discrete features in REE patterns of geological materials (Mc Lennan, 1994). In the present study, the low analytical uncertainty on $\log K_d^{REE}$ values from adsorption experiments (±2%) combined with the large amplitude between $\log K_d^{REE}$ values from different tetrad groups (e.g. 8.2% between $\log K_d^{Eu}{}_{inorganic}$ and $\log K_d^{Gd}{}_{inorganic}$ for the $NaNO_3$adsorption experiment) suggest that the tetrad effect is effective and not an artefact.

$Ce_{inorganic}$ anomalies, experessed as Ω(Ce) values, were all positive and almost constant over the 12 d of the experiment, ranging from 0.16 to 0.22 (Fig. 6). As with the log

$K_d^{REE_{inorganic}}$ values, these values are slightly less than the Ce anomaly values published by Ohta and Kawabe (2001) for similar pH conditions (around 1.7 time lower).

3.2. Comparison of REE adsorption kinetics and log $K_d^{REE_{organic}}$ and log $K_d^{REE_{inorganic}}$ at pH 5

The experimental results of log $K_d^{REE_{organic}}$ for La, Ce, Pr, and Sm are plotted in Fig. 4. The data show that the complexation of REE(III) by humic acid had large effects on both REE adsorption kinetics and K_d^{REE} equilibrium values. Time series variations of log $K_d^{REE_{organic}}$ values reveal that equilibrium was not reached before around 10 d when REE occurred as REE(III)-humate complexes (Fig. 4), against 10 h when dissolved REE were in solution as free metal ions (Fig. 2; Ohta and Kawabe, 2001). As regards to the partition coefficients, log K_d^{REE} values were lower in the two organic experiments as compared to the inorganic case, ranging from 3.4 to 3.5 in the $NaNO_3$ solution experiment and from 3.35 to 3.40 in the NaCl solution experiment against 3.3 to 4.2 in the inorganic run (Fig. 3). Ratios of $\log K_d^{REE_{organic}} / \log K_d^{DOC}$ were close to 1.0 indicating that the REE(III) and the humic acid remained bound to each other during interaction of the REE(III)-humate complexes with the MnO_2 surface.

The patterns of log $K_d^{REE_{organic}}$ differ markedly from those recovered during the inorganic experiments (compare Figs 3 and 5). Firstly, the organic patterns do not show the same conspicuous tetrad effect or "M" shape (Fig. 3). This general lack of a conspicuous "M" shape in the organic patterns is highly significant with regards to the adsorption mechanism(s) of the REE(III)-humate complexes onto MnO_2. We note that all the adsorption experiments

conducted so far between $REE(III)_{(aq)}$ and either MnO_2 or Fe oxyhydroxides yielded patterns of log K_d^{REE} that showed invariably convex tetrad effects (De Carlo et al., 1998, 2000; Bau, 1999; Ohta and Kawabe, 2001; Fig. 3). Secondly, a significant positive Ce anomaly was not observed in the patterns corresponding to the REE(III)-humate adsorption (Figs. 5 and 6).

3.3 Comparison of REE adsorption kinetics and log $K_d^{REE_{organic}}$ at pH 5 and 7.5

Sorption experiments of REE(III)-humate complexes onto MnO_2 at pH 7.5 are presented in Fig. 5. Adsorption kinetics are faster at pH 7.5 (4 d) than at pH 5 (10 d), equilibrium $\log K_d^{REE_{organic}}$ values being lower at pH 7.5 than pH 5. As with the experiments at pH 5, development of a positive Ce anomaly or tetrad effect is not observed at pH 7.5. Ratios of $\log K_d^{REE_{organic}} / \log K_d^{DOC}$ remained also close to 1.0 suggesting that the rise in pH had essentially no effect on the stability of the REE(III)-humate complexes upon adsorption

Note that the fairly large relative standard deviations obtained from the triplicate experiments conducted at pH 7.5 (Table 8; Appendix 2) is due to difficulties in pH regulation when pH approaches neutrality.

4. DISCUSSION

4.1. Mechanism of Ce anomaly and tetrad effect inhibition

REE adsorption experiments onto MnO_2 with REE(III) occurring as REE(III)-humate complexes evidence the same evolutionary features (i.e. slow-down of REE adsorption kinetics; inhibition of tetrad effect and Ce anomaly development) whatever the supporting

electrolyte ($NaNO_3$ or NaCl). A clear distinction appears between these results and those stemming out of the inorganic experiments (this study; Ohta and Kawabe, 2001). In this context, one key question is how does complexation of REE(III) by humic acid inhibit the development of a positive Ce anomaly at the surface of the MnO_2 oxides?

The lack of positive Ce anomalies in log K_d^{REE} patterns does not necesseraly mean that all the adsorbed Ce occurs as Ce(III). In Mn or Fe oxyhydroxides suspensions where REE occur as inorganic species, the development of a positive Ce anomaly is due to oxidative/scavenging which is the sum of (i) oxidation of Ce(III) into Ce(IV) and (ii) preferential sorption of Ce(IV).This decoupling of Ce(IV) from the REE(III) upon adsorption is due to the change in ionic charge and radius imposed by the oxidation process. However, cationic adsorption onto oxyhydroxides increases with increasing pH. In strong pH-conditions, Ce(IV) is present onto the oxyhydroxide surface, but hid in the large amount of REE(III) adsorbed, any positive Ce anomaly is developed despite the occurrence of Ce(IV). This effect of pH on Ce anomaly was studied by Bau (1999) for Fe hydroxide and by Ohta and Kawabe (2001) for MnO_2. According to Bau's (1999) results, the amount of extra Ce scavanged onto Fe hydroxide due to oxidation of Ce(III) to Ce(IV) could not be detected above a pH of ca. 5 (no occurrence of a mesurable positive Ce anomaly). As regards MnO_2, a positive Ce anomaly was still present at pH 7 - the highest pH value investigated by Ohta and Kawabe (2001) -, but the size of the anomaly was found to start decreasing above a pH of 6.5.

For REE-humate complex, Ce adsorption mechanism is complicated by the bound of REE to high molecular weight humate and be their distinct sportive properties - humate adsorbed at low pH (Avena and Koopal, 1999), aqueous trace metals adsorbed at high pH-. Humate are large polyfunctionnal macromolecules, potentially able to complex without selection hundreds of REE. This lack of selectivity among the REE group is consistent with the regular log K_d^{REE} patterns of REE-humate complexes (no sign for any preferential Ce

complexation). Both characteristics of humate – i.e. high complexation capacity; lack of Ce complexation selectivity – are strong obstacle to the preferential Ce(IV) adsorption necessary to develop positive Ce anomalies. This could be the main reason (rather than inhibition of Ce(III) oxidation) why positive Ce anomalies were not observed in experiments where REE occurred as REE(III)-humate complexes.

This "buffering" effect of humate on Ce/REE fractionation is confirmed by pH 5 and pH 7.5 experiments. Cation ligand complexes, denoted as ML (with M and L representing, the cation and the ligand respectively) can adsorb onto a solids ($\equiv S$) to form ternary surface complexes. These complexes could exist in two forms (i) $\equiv S-LM$ (cation linked to the mineral surface over the ligand) or (ii) $\equiv S-O-ML$ (ligand linked to the surface over the cation) (Schindler, 1990, Nowack and Sigg, 1996). The formation of both types of complexes depends on whether the surface groups of the oxide can participate in exchanging their OH^- with the cation-ligand complex. These reactions depend strongly on pH. When pH is lower than the solid pH_{zpc} (pH for which positive and negative charges occur in equal number) adsorption is of anionic type ($\equiv S-LM$). In pH 5-experiments, pH was slightly lower than the pH_{zpc} of the MnO_2 used in this study (5.8). Consequently, anionic adsorption occurred (eq. 4)

$$\equiv S-OH \; + \; REE\text{-}PHA \; \Leftrightarrow \equiv S-PHA\text{-}REE + OH^- \qquad (4)$$

In such a situation Ce was not in contact with the oxidative MnO_2 surface and Ce(III) was consistently not oxidized in Ce(IV) (no possibility of developping a positive Ce anomaly). In the second series of experiments, however pH was rise at 7.5, i.e. a value well above the pH_{zpc} of the MnO_2. Under such a situation, cationic adsorption could occur (eq. 5):

$$\equiv S-OH \; + \; REE\text{-}PHA \; \Leftrightarrow \equiv S\text{-}O\text{-}REE\text{-}PHA + H^+ \qquad (5)$$

In this case, Ce(III) could become oxidized, and Ce/REE fractionation could develop. However, it is clear from Figure 5 that no Ce/REE fractionation occurred in the experiments

at pH 7.5. The equilibrium time and $\log K_d^{REE_{organic}}$ values decrease is meaningful with regards to the REE-humate complex adsorption. The REE-humate complex seems to have the same behaviour onto solid surface than an 'uncomplexed' humate (decrease of adsorption rate at high pH). Unlike in the inorganic experiments where Ce and REE can adsorb onto MnO_2 surfaces independently from each other, REE (including Ce(IV)) are physically linked together by the humate molecule in the organic experiments. Ce can thus be oxidized by the MnO_2 surface. However, a positive anomaly cannot develop. The preferential Ce(IV) sorption cannot proceed due to binding of the entire REE pool to humate.

Finally, we are concerned by the lack of tetrad effect for the $\log K_d^{REE_{organic}}$ values in the patterns. It was suggested that the growth of convex tetrad effect may reflect the change of coordination state of the REE(III) adsorbed onto either MnO_2 or Fe oxyhydroxides (Bau, 1999; Ohta and Kawabe, 2001). Ohta and Kawabe (2001) hypothesized that REE(III) adsorbed onto MnO_2 are linked with hydroxyl ions, water molecules and oxygen bound with Mn(IV). According to these authors (op. cit.), this coordination would explain the increase of convex tetrad effect with pH, by the increasing proportion of hydroxyl ion bonding REE(III). When REE(III) are complexed by humic acid, interaction of the ternary complex thus formed with the MnO_2 surface occurs dominantly by the humate side, implying that a large part of the REE(III) pool is probably not directly bound to the MnO_2 surface. The presence of the lanthanide tetrad effect reveals that during the interaction of dissolved REE(III) with MnO_2, the behaviour of these elements cannot fully be described by differences between their ionic radii, requiring instead changes of the coordination state of the REE(III) adsorbed onto MnO_2. The latter mechanism would be hardly activated since REE (III) cannot directly interact with the MnO_2 surface in the organic experiment.

Moreover, the tetrad effect expresses the differences in Racah parameters for 4f electron repulsion between the pair of REE complexes. Ohta and Kawabe (2001) suggested

that Racah parameters in REE(III) ions decrease with increasing covalence of bonding of REE(III) with ligands. If REE-humate complexes are adsorbed onto MnO_2 as $\equiv S-O-ML$ (eq. 5, cationic adsoption), Racah parameters are smaller and, consequently, a conspicuous M-type tetrad effect should be observed. Thus, the lack of tetrad effect in the log $K_d^{REE_{organic}}$ patterns suggests that REE(III)-humate complexes is bound to MnO_2 by the humate side confirming the chemical mechanism of eq. 4.

4.3. Comparison with natural waters and inferences on the use of Ce anomaly as a redox proxy in paleosols.

Shallow organic-rich waters from several continental areas (e.g. western Europe and Africa) have been shown to be characterized by no, or only very small negative Ce anomalies despite the occurrence in these waters of strongly oxidizing conditions and of Mn oxides in associated aquifers (Viers et al., 1997; Braun et al., 1998; Dia et al., 2000; Gruau et al., 2003). Figure 8 presents Ω(Ce) vs. Mn and Ω(Ce) vs. DOC plots that illustrate both two characteristics. Particularly interesting are the data from the Kervidy-Naizin catchment in western France (Dia et al., 2000). As can be seen, the hydrochemical dataset from this catchment shows clear evidence of Mn oxidation and MnO_2 precipitation at the soil-water interface as revealed by the marked decrease of dissolved Mn concentrations; yet, Ω(Ce) decrease only very slightly (Fig. 8).

In their paper, Dia et al. (2000) stated that "*it is clear that the lack of Ce anomaly is a rather surprising feature given the redox sensitive chemistry of this element and the occurrence of seasonal redox variations"* in the Mercy wetland (i.e. the precise name of the site from which the Kervidy-Naizin waters were sampled). Taking into account the fact that Ce and REE do not occur as free metal ions in these waters, but occur predominantly as

dissolved and colloidal organic complexes, Dia et al. (2000) put forward two hypotheses to account for this lack of Ce anomalies: (i) either Ce precipitation and oxidation became impossible because of the complexation of Ce(III) by organic matter or, (ii) CeO_2 precipitated onto colloids being then considered as part of the solution. The experimental data reported in this study favour the first hypothesis, though showing that the true ultimate cause of the lack of Ce anomly development in these waters is more likely to be inhibition of prefrential Ce(IV) sorption rather than inhibition of Ce oxidation reaction

Another implication of the results of this study concerns the use of Ce anomalies in paleosols as paleoclimatic proxies. In the last two decades, many environmental proxies have been explored on paleaosol sequences, including Ce anomalies (Rankin and Child, 1976; Gallet et al., 1996; Braun et al. 1998). It was stated that the redox state of a paleosol at the time of its formation should correlate with climatic factors such as rainfall intensity or/and ambient atmospheric temperature. From a paleoclimatic point of view, it is indeed possible that wet periods led to the dominance of oxidizing conditions in paleosols due to the continuous recharge of the soil solution by oxygen-rich rainwater, a process which would stabilize Mn oxide phases in the weathering front. Considering solely the inorganic experimental results of Ohta and Kawabe (2001), one could then consider that both negative or positive Ce anomalies would be expected to occur in paleosols formed under such conditions, depending on whether the latter incorporated the stabilized Mn oxide phases (positive Ce anomaly) or contained secondary mineral phases precipitated from fluids in equilibrium with the Mn oxide solids (negative Ce anomaly). However, these new experimental results show that the complexation of REE(III) by humic substances - a process likely to occur during formation of organic-rich paleosols - could possibly destroy such a pattern by partially inhibiting the development of a positive Ce anomaly on soil Mn oxides, hence making Ce anomalies in paleosols a poor paleo(redox)climatic proxy. In previous

studies dedicated to test the occurrence of paleoclimatic proxies in the loess-paleosol sequences of China, Gallet et al. (1996) and Jahn et al. (2001) showed that the soils from these sequences yielded variable Ce anomalies, uncorrelated with well-established climatic proxies such as the magnetic susceptibility or the chemical index of alteration. In their 2001 paper, Jahn and co-workers failed to find any satisfactory explanation for this discrepancy in term of climatic variability or differences in pedogenetic or alteration intensity. Then, the interplay between variable redox conditions and REE(III) organic speciation may lead to complex REE patterns in paleosols which may not unambiguously reflect the climatic conditions at time of their genesis.

5. SUMMARY

Free REE(III) and REE(III)-humate complexes adsorption behaviour onto MnO_2 point out that humate complexation strongly modified the REE sorptive properties. Time-series experiments indicate that a stationary exchange equilibrium is reached within less than 10 h when dissolved REE(III) occurs as free and 10 d when REE occur as REE(III)-humate complexes. Humate complexation also resulted in an inhibition of positive Ce anomalies and M-type lanthanide tetrad effect development.

The strong REE complexation capacity of humate coupled to their inability to preferentially complex Ce prevent the preferential adsorption of Ce(IV) necessary to positive Ce anomalies development. As regards inhibition of the lanthanide tetrad effect is attributed the the anions adsorption of the REE-humate complex (eq. 4), REE(III)-humate adsorbed onto the MnO2 surface by the humate side. Under this condition, the changes in ionic radii required for the lanthanide terad effect to develop cannot proceed.

These new experimental data show that Ce anomalies may not be a reliable proxy of redox conditions in organic-rich waters or in precipitates formed in equilibrium with humic substances rich waters. These data help to explain why no, or insignificant negative Ce anomalies may be observed in shallow organic-rich groundwaters despite the development of strongly oxidizing conditions and the presence in the aquifer of MnO_2.

Acknowledgements. We thank the technical staff in Rennes for their assistance during the experimental and analytical work. Thierry Bataille from the XRD laboratory of Rennes University is acknowledged for his help in determining the MnO_2 cristallographic structure. This research was supported by the INSU-CNRS through Programme PNSE.

REFERENCES

AFNOR: 1994, *Qualité des Sols*, AFNOR, Paris, 250pp.

Aubert D., Stille P., Probst A., Gauthier-Lafaye F., Pourcelot L. and Del Nero M. (2002) Characterization and migration of atmospheric REE in soils and surface waters. *Geochim. Cosmochim. Acta* **66**, 3339-3350.

Avena M. J. and Koopal L. K. (1999) Kinetics of humic acid adsorption at solid-water interface. *Environ. Sci. Technol.* **33**, 2739-2744.

Bau M. (1999) Scavenging of dissolved yttrium and rare-earths by precipitating iron oxyhydroxydes: Experimental evidence for Ce oxidation, Y-Ho fractionation, and Lanthanide tetrad effect. *Geochim. Cosmochim. Acta* **63**, 67-77.

Biddau R., Cidu R. and Frau F. (2002) Rare-earth elements in water from the albitite-bearing granodiorites of Central Sardinia, Italy. *Chem. Geol.* **182**, 1-14.

Braun J. J., Viers J., Dupré B., Polvé M., Ndam J. and Muller J. P. (1998) Solid/liquid fractionation in the laterite system of Goyoum, East Cameroon: The implication for the present dynamics of the soil covers of the humid tropical regions. *Geochim. Cosmochim. Acta* **62**, 273-299.

Byrne R. H. and Li B. (1995) Comparative complexation behaviour of the rare earths. *Geochim. Cosmochim. Acta* **59**, 4575-4589.

Davranche M., Lacour S., Bordas F. and Bollinger J-C. (2003) An easy determination of the surface chemical properties of simple and natural solids. *J. Colloid Interf. Sci*. **80**, 76-78.

De Baar H. J. R., Bacon M. P. and Brewer P. G. (1983) Rare-earths distributions with a positive Ce anomaly in the western North Atlantic Ocean. *Nature* **301**, 324-327.

De Baar H. J. R., Bacon M. P., Brewer P. G. and Braland K. W. (1985) Rare-earths in the Pacific and Atlantic Ocean. *Geochim. Cosmochim. Acta* **49**, 1943-1959.

De Baar H. J. W., German C. R., Elderfield H. and Van Gaans P. (1988) Rare-earths element distributions in anoxic waters of the Cariaco Trench. *Geochim. Cosmochim. Acta* **52**, 1203-1219.

De Carlo E.H. and McMurthy G.M. (1992) Rare earth element geochemistry of ferromanganese crusts from the Hawaiian Archipelago. *Chem. Geol*. **95**, 235-240.

De Carlo E. H., Wen X.-Y., and Irving M. (1998) The influence of redox reactions on the uptake of dissolved Ce by suspended Fe and Mn oxide particles. *Aquatic Geochem.* **3**, 357-389.

De Carlo E.H., Wen X. Y. And Coven J. P. (2000). Rare earth element fractionation in hydrogenetic Fe-Mn crusts: The influence of carbonate complexation and phosphatization on Sm/Yb ratios. In *Marine authigenesis: From Global to Microbial* (Eds. C. R. Glenn, L. Prevot-Lucas and J. Lucas). SPM special, Vol 64, pp 271-285.

Dia A., Gruau G., Olivié-Lauquet G., Riou C., Molénat J. and Curmi P. (2000) The distribution of rare-earths in groundwater: Assessing the role of source-rock composition, redox changes and colloidal particles. *Geochim. Cosmochim. Acta* **24**, 4131-4151.

Elbaz-Poulichet F. and Dupuy C. (1999) Behaviour of rare-earths elements at the freshwater-seawater interface of two acid mine rivers : the Tinto and Odiel (Andalucia, Spain). *Appl. Geochem*. **14**, 1063-1072.

Elderfield H. (1988) The oceanic chemistry of the rare-earth elements. *Trans. R. Soc. London A* **325**, 105126

Elderfield H., Hawkesworth C.J., Greaves M.J., and Calvert S.E. (1981) Rare earth element geochemistry of oceanic ferromanganese nodules and associated sediments. *Geochim. Cosmochim. Acta* **45**, 513-528

Elderfield H. and Graves M. J. (1982) The rare-earths in seawater. *Nature* **296**, 214-219.

Elderfield H., Upstill-Goddard R. and Sholkovitz E. R. (1990) The rare-earth elements in rivers, estuaries, and coastal seas and their signifiance to the composition of ocean waters. *Geochim. Cosmochim. Acta* **54**, 971-991.

Gallet S., Jahn B.-M. and Torii M. (1996) Geochemical characterization of the Luochuan loess-paleosol sequence, China, and paleoclimatic implications. *Chem. Geol.* **133**, 67-88.

Goldberg E. D., Koide M., Schmitt R. A. and Schmith R. H. (1963) Rare-earth distribution in the marine environment. *J. Geophys. Res.* **68**, 4209-4217.

Gosselin D. C., Smith M. R., Lepel E. A., Laul J. C. (1992) Rare-earth elements in chloride-rich groundwater, Palo Duro Basin, TX, ASA. *Geochim. Cosmochim. Acta* **56**, 1495-1505.

Gruau, G., Dia, A., Olivié-Lauqué, G., Davranche, M., Pinay, G., Petitjean, P., Henin, O. and Le Coz-Bouhnik, M (2004) Controls on the distribution of rare earth elements in shallow groundwaters. *Wat. Res*. *(in press)*

Holser W. T. (1997) Evaluation of the application of rare-earths elements to paleooceanography. *Paleogeol. Paleoclim. Paleoecol.* **132**, 309-323.

Jahn B.-M., Gallet S., Han J. (2001) Geochemistry of the Xining, Xifeng and Jixian sections, Loess Plateau of China: eolian dust provenance and paleosol evolution during the last 140 ka. *Earth Planet. Sci. Lett.* **178**, 71-94.

Johannesson K. H. and Lyons W. B. (1994) The rare-earth elements geochemistry of Monolake water and the importance of carbonate complexing. *Limn. Oceanogr*. **39**, 1141-1154.

Johannesson K. H. and Lyons W. B. (1995) Rare-earth elements geochemistry of Colour lake, an acidic freshwater lake on Axel Heiberg Island, Northwest Territories, Canada. *Chem. Geol.* **119**, 209-223.

Johannesson K. H., Stetzenbach K. J., and Hodge V. F. (1995) Speciation of the rare earth element neodymium in groundwaters of the Nevada Test Site and Yucca Mountain and implications for actinide solubility. *Appl. Geochem.* **10**, 565-572

Koeppenkastrop D. and De Carlo E. H. (1992) Sorption of rare-earth elements from seawater onto synthetic mineral particles: An experimental approach. *Chem. Geol.* **95**, 251-263.

Koeppenkastrop D. and De Carlo E. H. (1993) Uptake of rare earth elements from solution by metal oxides. *Environ. Sci. Technol.* **27**, 1796-1802.

Kuss J., Garbe-Schönberg C-D. and Kremling K. (2001) Rare-earth elements in suspended particulate material of North Atlantic surface waters. *Geochim Cosmochim. Acta* **65**, 187-199.

Langmuir D. (1997) *Aqueous Environmental Geochemistry.* Prentice Hall, Upper Saddle River, New Jersey.

Leybourne M. I., Goodfellow W. D., Boyle D. R. and Hall G. M. (2000) Rapid development of negative Ce anomalies in surface waters and contrasting REE patterns in groundwaters associated with Zn-Pb massive sulphide deposits. *Appl. Geochem*. **15**, 695-723.

McLennan S.M. (1994) Rare earth element geochemistry and the 'tetrad' effect. *Geochim. Cosmochim. Acta* **58**, 2025-2033.

Macleod K. G. and Irving A. J. (1996) Correlation of cerium anomalies with indicators of paleoenvironment. *J. Sedim. Res.* **66**, 948-955.

Moffet J. W. (1990) Microbially mediated cerium oxidation in sea water. *Nature* **345**, 421-423.

Möller P., Paces T., Dulski P. and Morteani G. (2002) Anthropogenic Gd in surface water drainage system and the water supply of the city of Prague, Czech republic. *Environ. Sci. Technol.* **36**, 2387-2394.

Morad S. and Felitsyn S. (2001) Identification of primary Ce-anomaly signature in fossil biogenic apatite: implication for the Cambrian oceanic anoxia and phosphogenesis. *Sed. Geol*. **143**, 259-264.

Nowack B. and Sigg L. (1996) Adsorption of EDTA and metal-EDTA complexes onto Goethite. *J. Colloid Interface Sci.* **177**, 106-121.

Ohta A. and Kawabe I. (2000) Rare earth element partitioning between Fe oxyhydroxide precipitates and aqueous NaCl solutions doped with $NaHCO_3$: Determinations of rare earth element complexation constants with carbonate ions. *Geochem. J.* **34**, 439-454.

Ohta A. and Kawabe I. (2001) REE(III) adsorption onto Mn dioxide (δ-MnO_2) and Fe oxyhydroxide: Ce(III) oxidation by δ-MnO_2. G*eochim. Cosmochim. Acta.* **65**, 695-703.

Picard S., Lécuyer C., Barrat J-A., Garcia J-P., Dromart G., and Sheppard S.M.F. (2002) Rare earth element contents in Jurassic fish and reptile teeth and their potential relation to seawater composition (Anglo-Paris Basin, France and England). *Chem Geol* **186**, 1-16.

Piper D.Z. (1974) Rare earth elements in ferromanganese nodules and other marine phases. *Geochim. Cosmochim. Acta* **38**, 1007-1022.

Rankin P.C. and Child C. W. (1976) Rare-earth elements in iron-maganese concretions from some New Zealand soils. *Chem. Geol.*, **18**, 55-64.

Schindler P.W. (1990) Co-adsorption of Metal Ions and Organic Ligands: Formation of Ternary Surface Complexes. In *Mineral-Water Interface Geochemistry* (Eds. M. F. Hochella and A.F. White). Mineralogical Soc. Of Am., Whashington D.C., Vol 23, pp.

Sholkovitz E. R. (1995) The aquatic chemistry of rare earth elements in rivers and estuaries. *Aquat. Geochem*. **1**, 1-34.

Smedley P. L. (1991) The geochemistry of rare earth elements in groundwater from the Carnmennellis area, southwest England. *Geochim. Cosmochim. Acta* **55**, 2767-2779.

Tang J., Johannesson K. H. (2003) Speciation of rare earth elements in natural terrestrial waters/ Assesing the role of dissolved organic matter from the modeling approach. *Geochim. Cosmochim. Acta* **67**, 2321-2339.

Takahashi Y., Minai Y., Ambe S., Makide Y. and Ambe F. (1997) Simultaneous determination of stability constants of humate complexes with various metal using multitracer technique. *Sci. Total Environ.* **198**, 61-71.

Takahashi Y., Minai Y., Makide Y. and Ambe F. (1999) Comparison of adsorption behavior of multiple imorganic ions on kaolinite and silica in the presence of humic acid using the multitracer technique. *Geochim. Cosmochim. Acta* **63**, 815-836.

Van Middlesworth P. E., Wood S. A. (1998) The aqueous geochemistry of the rare elements and yttrium. Part 7. REE, Th and U contents in thermal springs associated with the Idaho batholit. *Appl. Geochem.* **13**, 861-884.

Vermeer A. W. P., Van Riemdjik W. H. and Koopal L. K. (1998) Adsorption of humic acid to mineral particles. 1. Specific and electrostatic Interactions. *Langmuir* **14**, 2810-2819.

Viers J., Dupré B., Polvé M., Schott J., Dandurand J-L. and Braun J-J. (1997) Chemical weathering in the drainage basin of a tropical watershed (Nsimi-Zoetele site, Cameroon): Comparison between organic-poor and arganic-rich waters. *Chem. Geol*. **140**, 181-206.

Wright J., Schrader H. and Holser W. T. (1987) Paleoredox variations in ancient oceans recorded by rare-earth elements in fossil apatite. *Geochim. Cosmochim. Acta* **51**, 631-644.

Yan X. P., Kerrich R. and Hendry M. J. (2001) Distribution of the rare earth elements in porewater from a clay-rich aquitard sequence, Saskatchewan, Canada. *Chem. Geol.* **176**, 151-172.

Yeghicheyan D., Carignan J., Valladon M., Bouhnik-Le Coz M., Le Cornec F., Castrec-Rouelle M., Robert M., Aquilina L., Aubry E., Churlaud C., Dia A., Deberdt S., Dupré B., Frédier R., Gruau G., Hénin O., De Kersabiec A-M., Petitjean P. and Serrat E. (2002) A compilation of some trace elements measured in natural river water standard SLRS-4 (NRC-CNRC). *Geostand. Newslett.*, **25**, 465-474.

FIGURES CAPTIONS

Fig. 1. Purification procedure of Aldrich humic substances.

Fig. 2. Equilibrium time of Log $K_d^{REE\ inorganic}$ in the suspension of MnO_2 and NaCl (a) or $NaNO_3$ (b) at pH 5, expressing the partitioning of 5 ppb REE between 100 mg MnO_2 and 1000 mL water within 2 weeks

Fig. 3. Log $K_d^{REE\ inorganic}$ patterns between MnO_2 suspension and NaCl or $NaNO_3$ aqueous solution plotted vs. increasing atomic number within REE series. Initial concentration of each REE was 5 ppb and solid phase concentration was 100 $mg.L^{-1}$. Errors bars correspond to σ for two replicates, some errors bars are within the symbol size.

Fig. 4. Equilibrium time of log $K_d^{REE\ organic}$ in the suspension of MnO_2 and NaCl (a), $NaNO_3$ (b) at pH 5 and NaCl (c) at pH 7.5 aqueous solutions, expressing the partitioning of REE-humate complexes between 100 mg solid and 1000 mL water within 3.5 weeks

Fig. 5. Log $K_d^{REE\ organic}$ pattern in the suspension of MnO_2 and NaCl or $NaNO_3$ at pH 5 and 7.5. Errors bars correspond to σ for three replicates, some errors bars are within the symbol size.

Fig. 6. Time variation of Ω(Ce) in the suspension of MnO_2 and NaCl or $NaNO_3$ at pH 5 expressing the Ce anomaly development. Errors bars corresponds to σ for two replicates in

inorganic and three replicates in organic experiments, some errors bars are within the size of the datum symbol.

Fig. 7. Relationships between Ω(Ce), DOC and Mn concentrations in organic-rich, soil waters from selected catchments from Western Europe, Pleine-Fougères and Kervidy-Naizin wetland. The dataset from the Kervidy-Naizin catchments was particularly meaningful as no, or only slight variation of the Ω(Ce) occurred in these soil waters despite the evidence of Mn oxidation and precipitation as showed by the marked decrease of dissolved Mn concentrations and increase of Eh data. Data sources: Dia et al. (2000); Gruau et al. (2004).

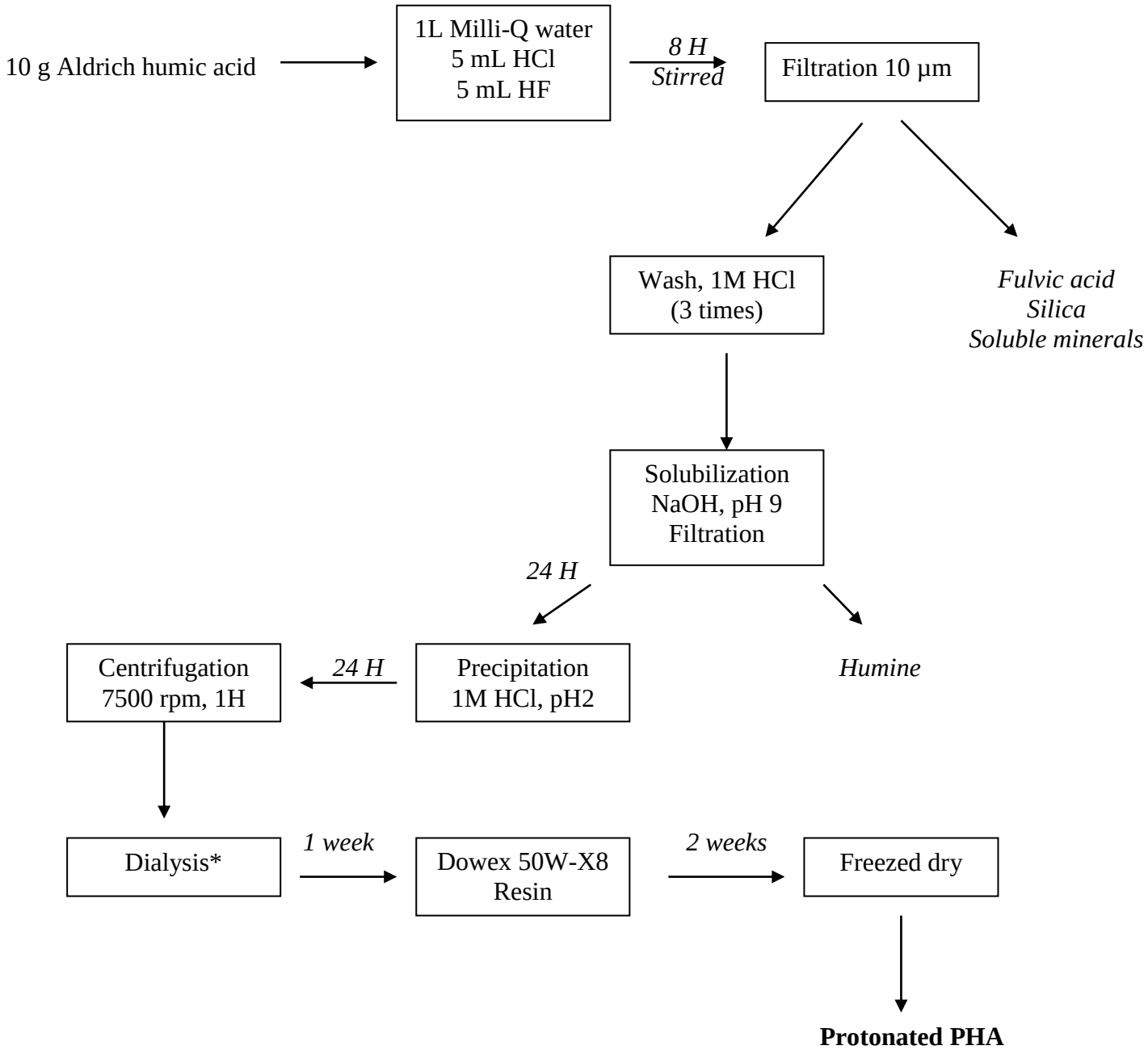

*: until the solution resistance equals before and after dialysis

Fig. 1.

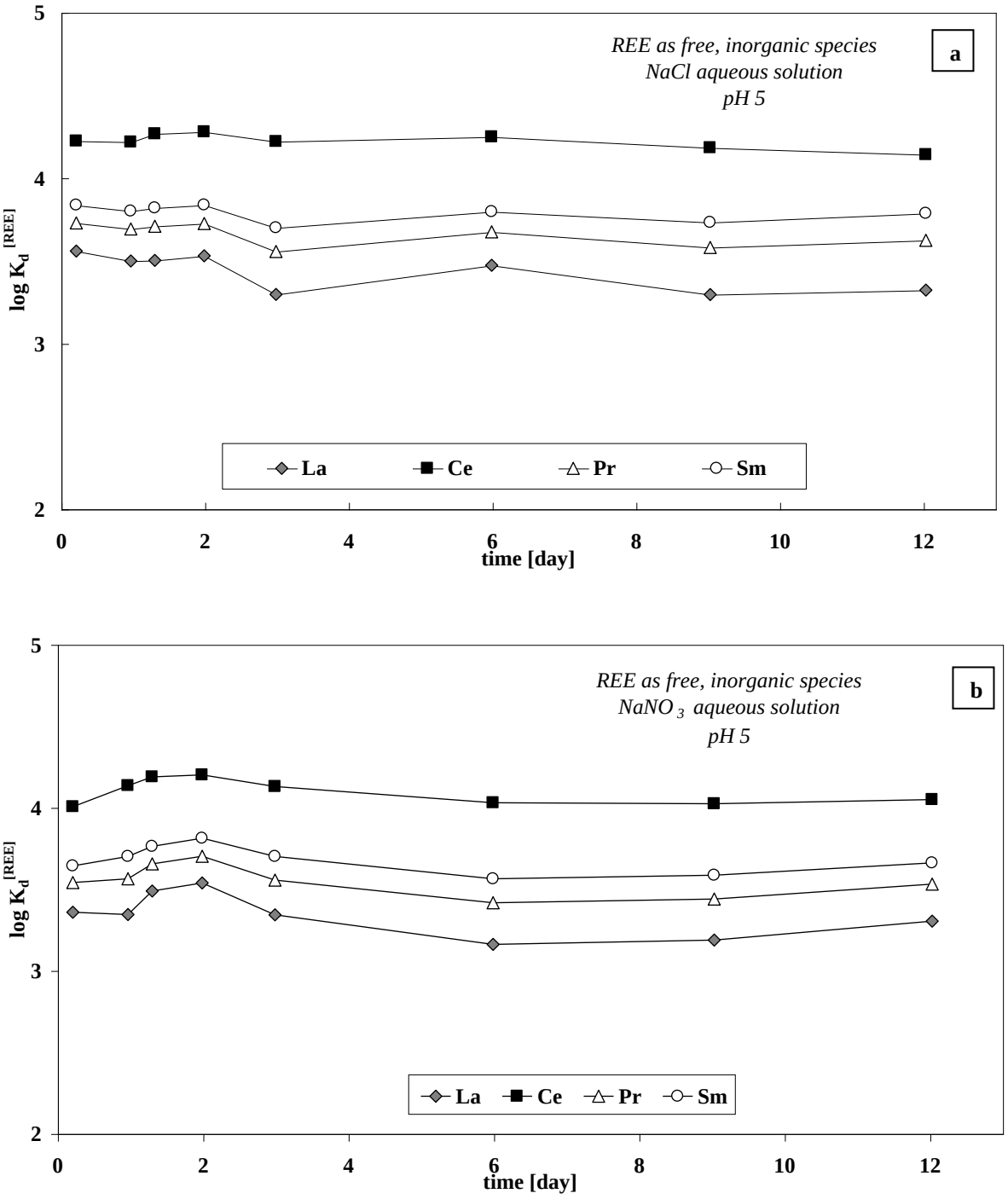
a
REE as free, inorganic species
NaCl aqueous solution
pH 5
log K_d [REE]
time [day]
La
Ce
Pr
Sm
b
REE as free, inorganic species
NaNO 3 aqueous solution
pH 5
log K_d [REE]
time [day]
La
Ce
Pr
Sm

Fig. 2.

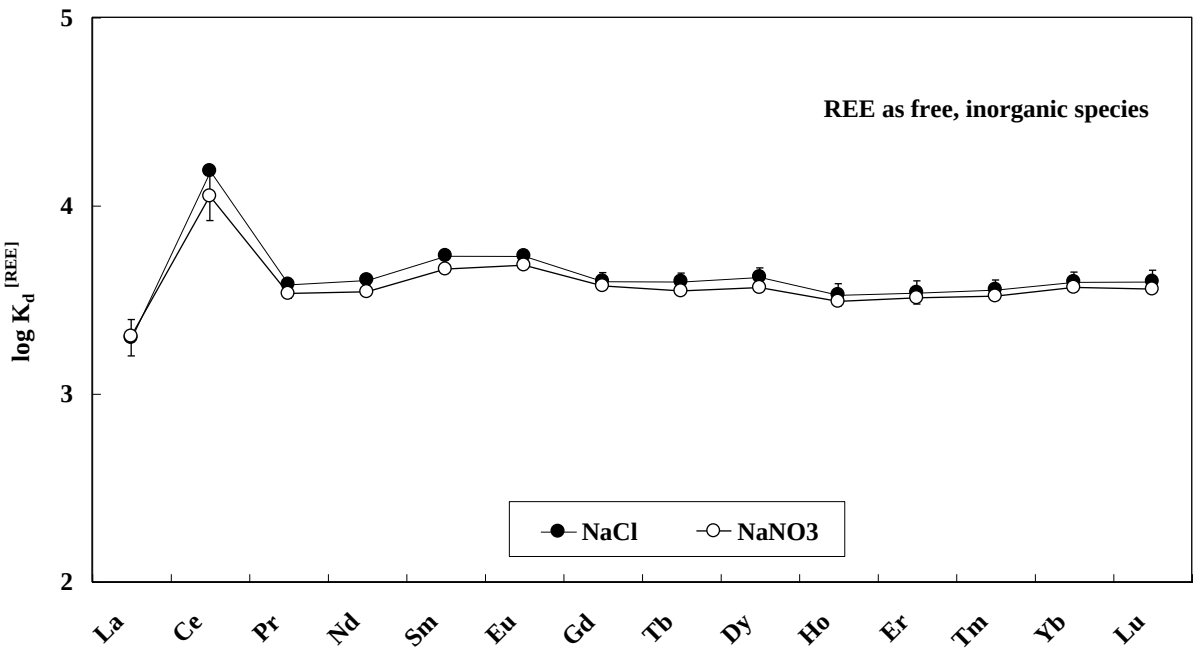
REE as free, inorganic species
log K_d [REE]
5
4
3
2
NaCl
NaNO3
La
Ce
Pr
Nd
Sm
Eu
Gd
Tb
Dy
Ho
Er
Tm
Yb
Lu

Fig. 3.

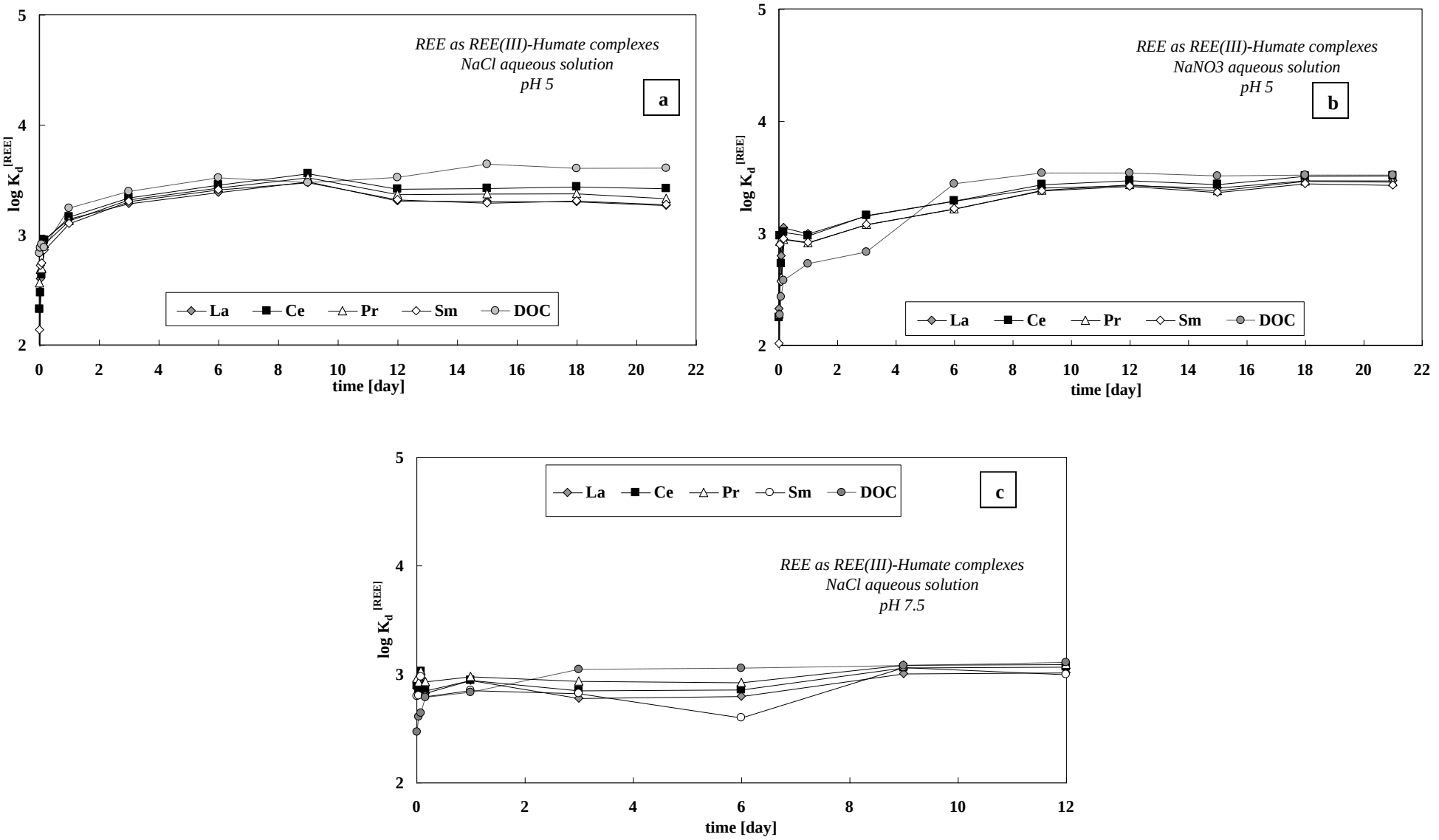
REE as REE(III)-Humate complexes
NaCl aqueous solution
pH 5
a
log K_d [REE]
time [day]
La
Ce
Pr
Sm
DOC
REE as REE(III)-Humate complexes
NaNO3 aqueous solution
pH 5
b
log K_d [REE]
time [day]
La
Ce
Pr
Sm
DOC
c
REE as REE(III)-Humate complexes
NaCl aqueous solution
pH 7.5
log K_d [REE]
time [day]
La
Ce
Pr
Sm
DOC

Fig. 4.

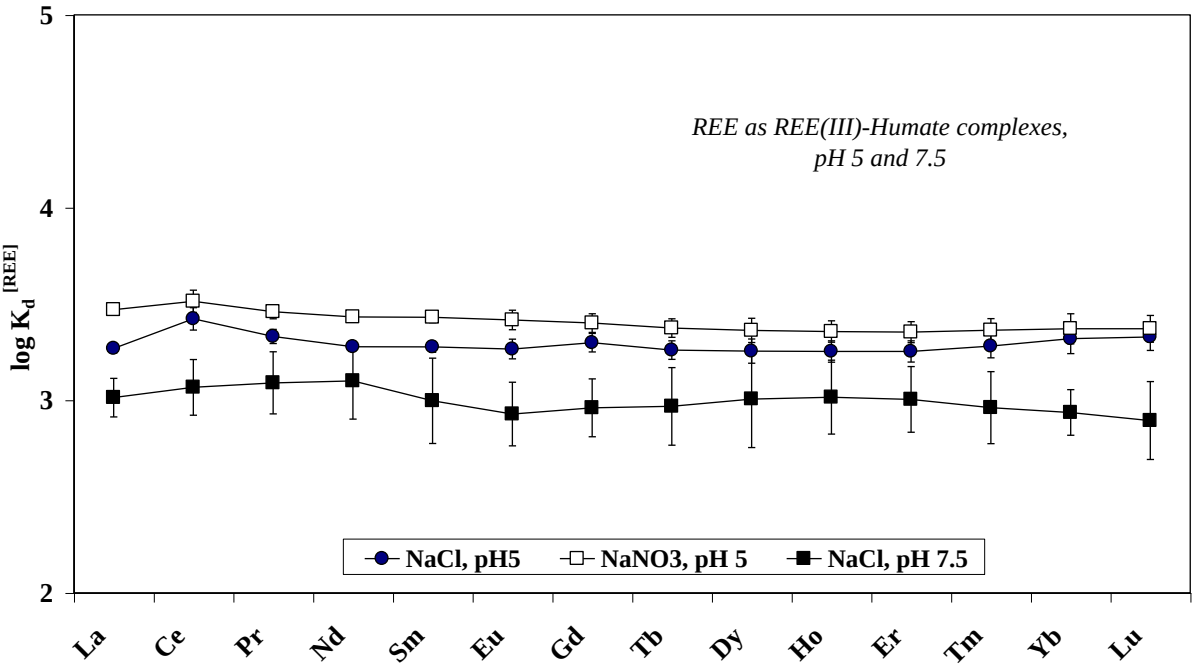
REE as REE(III)-Humate complexes,
pH 5 and 7.5
log K_d [REE]
5
4
3
2
NaCl, pH5
NaNO3, pH 5
NaCl, pH 7.5
La
Ce
Pr
Nd
Sm
Eu
Gd
Tb
Dy
Ho
Er
Tm
Yb
Lu

Fig. 5.

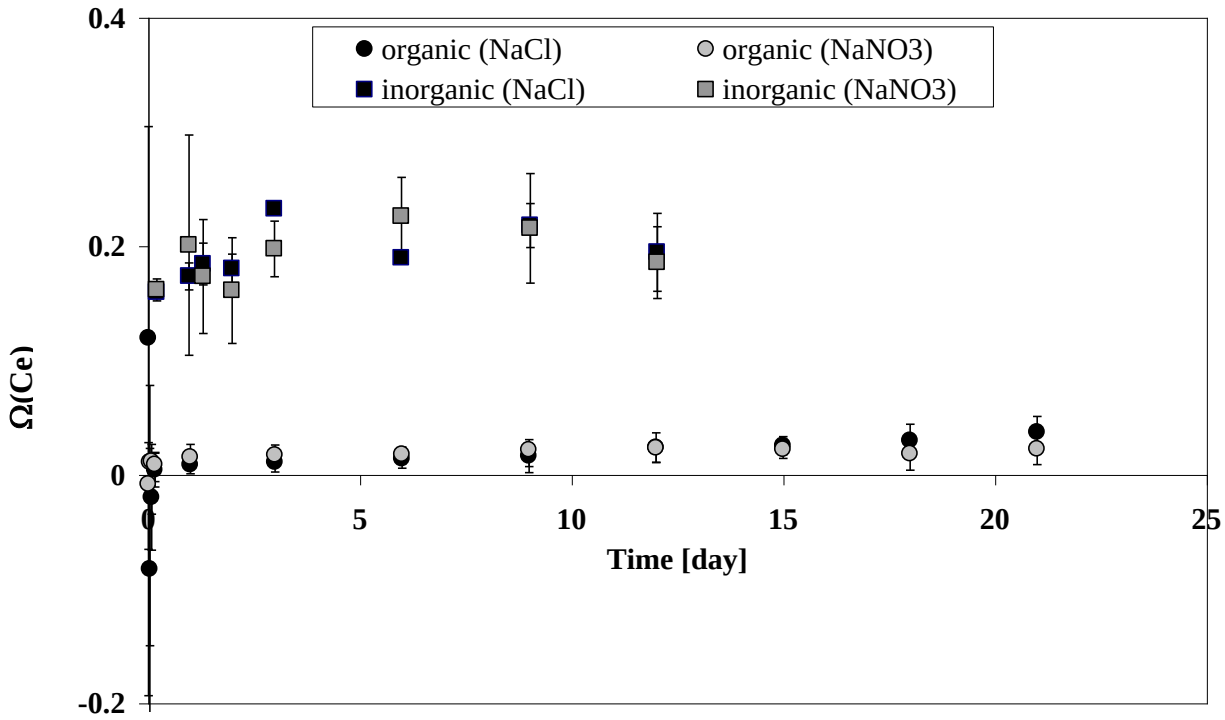
0.4
0.2
0
-0.2
Ω(Ce)
0
5
10
15
20
25
Time [day]
organic (NaCl)
organic (NaNO3)
inorganic (NaCl)
inorganic (NaNO3)

Fig. 6.

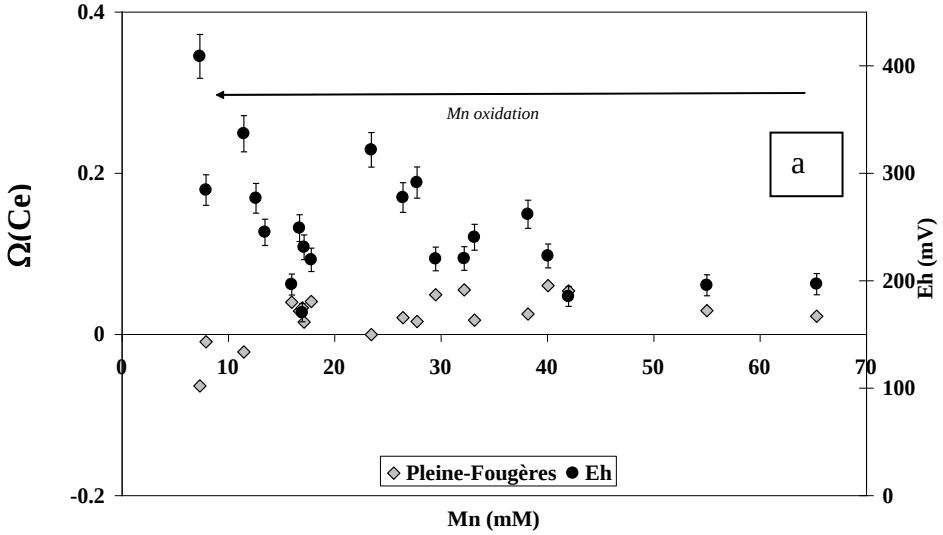
Mn oxidation
a
Ω(Ce)
Eh (mV)
Mn (mM)
Pleine-Fougères
Eh

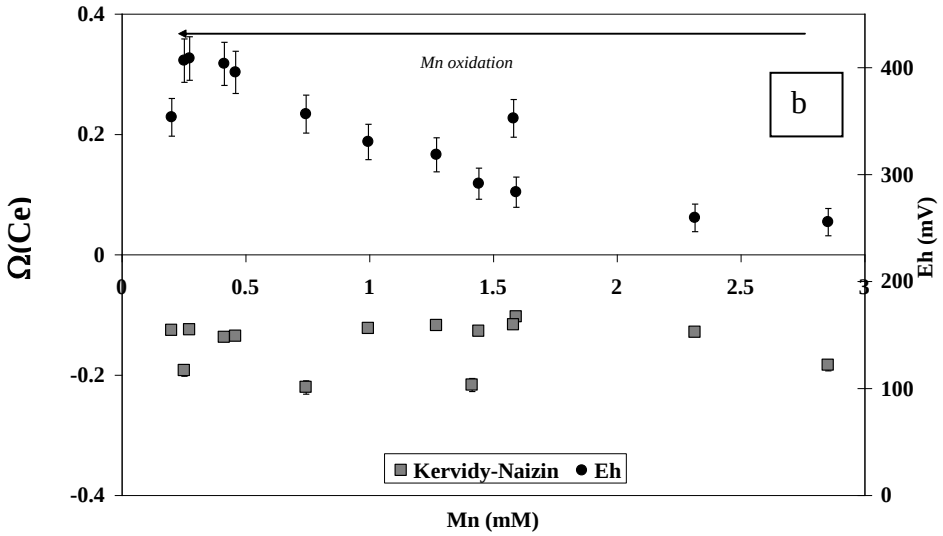
Mn oxidation
b
Ω(Ce)
Eh (mV)
Mn (mM)
Kervidy-Naizin
Eh

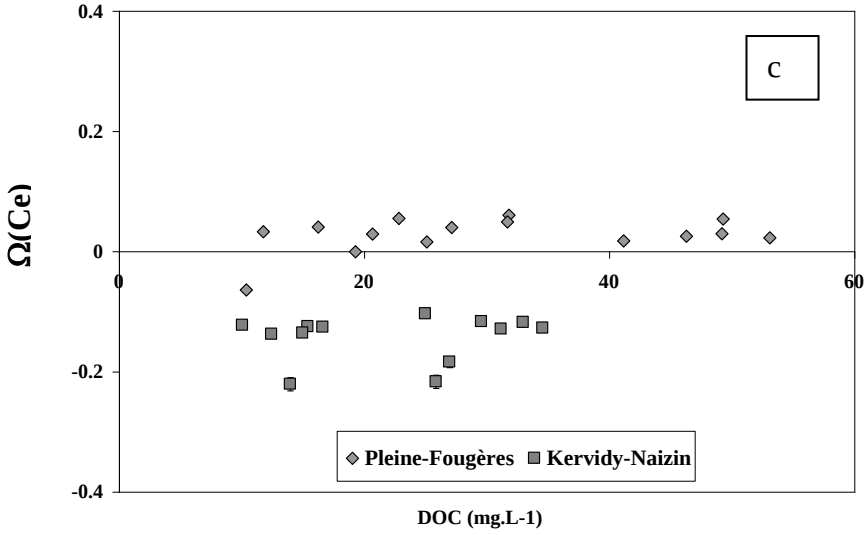
c
Ω(Ce)
DOC (mg.L-1)
Pleine-Fougères
Kervidy-Naizin

Fig.7.

Appendix 1 – Mass analyses and instrumental errors

Rare earth concentrations were determined using an Agilent Technologies^{TM} HP4500 ICP-MS Normal plasma conditions were used, with the instrumental parameters reported in Table 1.

Table 1. Instrumental and data acquisition parameters

RF power	1360 W
Plasma gas flux	15 L/min
Auxiliary gas flux	1.0 L/min
Carrier gas flux	1.13 L/min
Nebulizer type	Cross-flow
Spray chamber temperature	2°C
Integration time	3 sec/mass
CeO^+/Ce^+	0.6 %
Ce^{++}/Ce^+	1%

Quantitative analyses were performed using a conventional external calibration procedure. Three external standard solutions displaying REE concentrations similar to those of the samples analysed in this study were prepared from a multi-REE standard solution (Accu Trace^{TM} Reference,10 mg.L^{-1}, USA). Indium was added to all samples as an internal standard at a concentration level of 0.87 μM (100 ppb) to correct for instrumental drift and possible matrice effects. Indium was also added to external standard solutions. Calibration curves were calculated from measured REE/Indium intensity ratios.

Detection limits (DL) of the Agilent Technologies ICP-MS set up at Rennes University (Table2) were calculated using the following equation:

$$DL(pmol.L^{-1}) = \frac{3SD.C}{S-B} \quad (5)$$

where SD is the standard deviation obtained during instrumental blank measurements, C the REE concentration of a standard solution (between 29 and 36 pM depending of the REE), S and B, the ion counts obtained during standard solution and instrumental blank analyses, respectively.

Table 2. Detection limits and chemical blanks (in pM) measured during the course of this study

Isotope	DL	Chemical Blanks
La 139	1.15	4.37
Ce 140	3.21	5.71
Pr 141	0.64	2.35
Nd 146	3.54	7.28
Sm 147	5.52	0.64
Eu 153	0.92	0.76
Gd 158	2.67	2.07
Tb 159	0.38	1.50
Dy 163	1.29	2.76
Ho 165	0.49	1.08
Er 166	1.26	0.88
Tm 169	0.59	1.27
Yb 174	1.44	1.14
Lu 175	0.51	0.85

DL: detection limits

Chemical blanks of individual REE were all lower than 10 pM which is negligible (Table 2), being by three to four orders of magnitude lower than concentrations measured in the synthetic solutions used in the adsorption experiments.

Isobaric interferences due to the formation and ionisation of oxides and/or hydroxides in the ICP-MS can alter Sm, Eu, Gd and Tb concentration determination. The interference list is

given in Table 3 along with the equations used in our laboratory to correct REE concentrations from this potential error source. Note that Ce and its neighbours La and Pr - and thus the calculation of the Ce anomaly - are not affected by isobaric interference problems. There was no need for BaO and/or BaOH corrections onto Eu and Sm as our synthetic solutions did not contain any Ba.

Table 3. Summary of isobaric interferences encountered during REE analysis and correction equations used at Rennes University to correct measured concentrations from this effect

Isotope	Interference	Corrections
$^{147}\mathbf{Sm}^{+}$	$^{130}BaOH^{+}$	negligible
$^{153}\mathbf{Eu}^{+}$	$^{137}BaO^{+}$; $^{136}BaOH^{+}$	$Eu[153] = \mathrm{Int}[153] - \frac{^{153}(\mathrm{BaO, BaOH})}{^{137}\mathrm{Ba}} \times \mathrm{Int}[137]$
$^{158}\mathbf{Gd}^{+}$	$^{142}CeO^{+}$; $^{142}NdO^{+}$; $^{141}PrOH^{+}$	$\mathrm{Gd}[158]=\mathrm{Int}[158]-\frac{^{158}(\mathrm{Pr}\,OH)}{^{141}\mathrm{Pr}}\times\mathrm{Int}[141]-\frac{^{158}(CeO)}{^{140}Ce}\times\mathrm{Int}[140]-\frac{^{158}(NdO)}{^{142}Nd}\times\mathrm{Int}[142]$
$^{159}\mathbf{Tb}^{+}$	$^{143}NdO^{+}$	$\mathrm{Tb}[159] = \mathrm{Int}[159] - \frac{^{159}(NdO)}{^{143}Nd} \times \mathrm{Int}[143]$

Amplitude and efficiency of the Gd and Tb corrections can be evaluated from Table 4 where measured and corrected concentrations of Gd and Tb obtained for the SLRS-4 water geostandard are pooled together. Correction amplitudes are moderate, being 6% for Gd and only 2% for Tb, with the corrected values being in both cases by ≤2.5% within the range of the reference values published for the SLRS-4 water geostandard (Yeghicheyan et al.. 2001). These values should be regarded as maximum values for the results presented here as the ratios of

[Interfering Element]/[Interfered Element] are close to unity in our synthetic solutions against 10 to 65 in the SLRS-4 geostandard.

Table 4. Amplitude and efficiency of oxyde and hydroxide corrections on Gd and Tb during analysis of SLRS-4 water standard. Concentrations are in nM.

Isotope	Reference values*	Measured values	Corrected values	Correction (%)
Gd 158	0.210	0.228	0.213	6.4
Tb 159	0.026	0.026	0.026	2.4

** Yeghicheyan et al. (2001)*

Table 5. Replicates analyses (n=10) of multi-REE standard solution (Accu Trace™ Reference, USA). Concentrations are in nM.

Isotope	Standard REE 1 (2.5 nM)		Standard REE 2 (5.1 nM)	
	mean	rsd	mean	rsd
La 139	2.49	0.5	5.10	0.6
Ce 140	2.49	0.7	5.11	0.7
Pr 141	2.49	1.0	5.12	0.6
Nd 146	2.50	0.5	5.07	0.7
Sm 147	2.49	0.6	5.08	0.4
Eu 153	2.50	0.3	5.08	0.5
Gd 158	2.50	1.0	5.10	1.0
Tb 159	2.48	0.9	5.10	0.5
Dy 163	2.47	0.6	5.09	0.5
Ho 165	2.47	0.7	5.08	0.3
Er 166	2.48	0.4	5.06	0.5
Tm 169	2.47	0.6	5.06	0.4
Yb 174	2.47	0.6	5.09	0.6
Lu 175	2.46	0.8	5.07	0.5

rsd: relative standard deviation

Finally, the overall validity of the analytical procedure can be checked from Table 5 where replicates analyses (n=10) of multi-REE standard solution (Accu Trace™ Reference, USA) are reported and from Table 6 where concentrations of the SLRS-4 standard measured during the course of this study are compared with published reference values (Yeghicheyan et al., 2001). Altogether, these two tables show that the instrumental error on REE analysis in our laboratory is < ±2%.

Table 6. Comparison of the analytical accuracy of the Agilent Technology™ HP4500 ICP-MS set up at Rennes University against published reference values of the SLRS-4 water geostandard. Concentrations are in nM.

Isotope	mean (n=13)	reference concentrations
La 139	2.069	2.066
Ce 140	2.548	2.569
Pr 141	0.493	0.492
Nd 146	1.842	1.865
Sm 147	0.371	0.382
Eu 153	0.055	0.053
Gd 158	0.219	0.217
Tb 159	0.027	0.027
Dy 163	0.143	0.149
Ho 165	0.028	0.028
Er 166	0.081	0.080
Tm 169	0.011	0.010
Yb 174	0.068	0.069
Lu 175	0.011	0.011

Appendix 2 – Reproducibility of adsorption experiments

Equilibrium log K_d^{REE} values obtained during duplicate and triplicate experiments conducted in order to determine the overall exeperimental uncertainties of the method used in

this study are presented in Tables 7 (REE(III) occurring as free, inorganic species) and 8 (REE(III) as REE(III)-Humate complexes). The two tables show that the overall experimental uncertainties on the Log K_d^{REE} values discussed in this paper is better than ±10%.

Equilibrium log K_d^{DOC} values were also monitored in the adsorption experiments using REE as REE(III)-humate coomplexes. Table 9 shows that the overall analytical uncertainties obtained on this parameter as determined from triplicate run results is better than ±10%.

Table 7. Reproducibility of log K_d(REE, inorganic) at pH 5.

	inorganic, NaCl, pH 5				**inorganic, $NaNO_3$, pH 5**			
	A	**B**	**mean**	**rsd**	**A**	**B**	**mean**	**rsd**
La	3.15	3.50	3.32	7.46	3.32	3.29	3.30	0.45
Ce	4.07	4.22	4.14	2.62	4.14	3.96	4.05	3.23
Pr	3.54	3.71	3.63	3.48	3.55	3.51	3.53	0.71
Nd	3.57	3.73	3.65	3.16	3.55	3.53	3.54	0.43
Sm	3.71	3.86	3.79	2.85	3.67	3.66	3.66	0.19
Eu	3.73	3.86	3.80	2.54	3.68	3.68	3.68	0.02
Gd	3.59	3.76	3.68	3.40	3.58	3.56	3.57	0.38
Tb	3.58	3.75	3.67	3.35	3.55	3.55	3.55	0.03
Dy	3.60	3.76	3.68	3.07	3.56	3.57	3.56	0.28
Ho	3.49	3.70	3.59	4.15	3.49	3.49	3.49	0.14
Er	3.50	3.71	3.61	4.07	3.52	3.50	3.51	0.26
Tm	3.52	3.73	3.62	3.98	3.53	3.51	3.52	0.40
Yb	3.57	3.75	3.66	3.55	3.57	3.56	3.56	0.25
Lu	3.56	3.76	3.66	3.77	3.56	3.55	3.56	0.07

rsd: relative standard deviation

Table 8. Reproducibility of log K_d(REE, organic) at pH 5 and 7.5

	Organic, NaCl, pH 7.5					Organic, NaCl, pH 7.5					Organic, $NaNO_3$, pH 5				
	A	**B**	**C**	**mean**	**rsd**	**A**	**B**	**C**	**mean**	**rsd**	**A**	**B**	**C**	**mean**	**rsd**
La	3.26	3.25	3.29	3.27	0.7	3.11	3.01	2.91	3.01	3.3	3.26	3.25	3.29	3.47	0.66
Ce	3.49	3.37	3.41	3.42	1.7	3.21	3.07	2.92	3.07	4.7	3.49	3.37	3.41	3.51	1.65
Pr	3.37	3.29	3.33	3.33	1.1	3.26	3.07	2.94	3.09	5.2	3.37	3.29	3.33	3.46	1.06
Nd	3.28	3.26	3.29	3.28	0.6	3.27	3.15	2.88	3.10	6.4	3.28	3.26	3.29	3.43	0.53
Sm	3.31	3.26	3.26	3.28	0.9	3.15	3.09	2.74	3.00	7.4	3.31	3.26	3.26	3.43	0.81
Eu	3.27	3.21	3.31	3.27	1.6	3.09	2.92	2.76	2.93	5.6	3.27	3.21	3.31	3.42	1.49
Gd	3.31	3.25	3.34	3.30	1.5	3.13	2.91	2.84	2.96	5.1	3.31	3.25	3.34	3.40	1.42
Tb	3.25	3.22	3.31	3.26	1.5	3.13	3.04	2.74	2.97	6.8	3.25	3.22	3.31	3.37	1.42
Dy	3.25	3.19	3.32	3.25	1.9	3.16	3.14	2.72	3.01	8.3	3.25	3.19	3.32	3.36	1.88
Ho	3.21	3.23	3.32	3.25	1.7	3.17	3.08	2.80	3.02	6.4	3.21	3.23	3.32	3.36	1.65
Er	3.21	3.24	3.31	3.25	1.7	3.15	3.05	2.81	3.00	5.7	3.21	3.24	3.31	3.35	1.64
Tm	3.24	3.25	3.35	3.28	1.9	3.15	2.96	2.78	2.96	6.3	3.24	3.25	3.35	3.36	1.81
Yb	3.27	3.28	3.41	3.32	2.4	3.04	2.96	2.81	2.94	4.0	3.27	3.28	3.41	3.37	2.32
Lu	3.29	3.29	3.41	3.33	2.1	3.03	3.00	2.66	2.89	7.0	3.29	3.29	3.41	3.37	2.07

rsd: relative standard deviation

Table 9. Reproducibiliy of log K_d^{OC} at pH 5 et 7.5. See text for explanations

	A	**B**	**C**	**mean**	**rsd**
NaCl, pH 5	3.46	3.53	3.56	3.52	1.4
$NaNO_3$, pH 5	3.56	3.74	3.52	3.61	3.2
NaCl, pH 7.5	3.36	3.00	2.96	3.11	7.2

r.s.d. relative standard deviation